EXPERIMENTAL RESULTS OF BREAKING WAVE IMPACT ON A VERTICAL WALL WITH AN OVERHANGING HORIZONTAL CANTILEVER SLAB

Dogan Kisacik[1], Peter Troch[1] and Philippe Van Bogaert[1]

Physical experiments (at a scale of 1/20) are carried out using a vertical wall with horizontal cantilevering slab. Tests are conducted for a range of values of water depth, wave period and wave height. A parametric analysis of measured forces (F_h and F_v) both on the vertical and horizontal part of the scaled model respectively is conducted. The highest impact pressure and forces are measured in the case of breaking waves with a small air trap. Maximum pressures are measured around SWL and at the corner of the scaled model. The horizontal part of the scaled model is more exposed to impact waves than the vertical part. F_h and F_v are very sensitive for the variation of water depth (h_s) and wave height (H) while variation of wave period (T) has a rather limited effect.

Keywords: Vertical walls; breaking wave impact; impact pressure and force

INTRODUCTION

The growth of world trade requires the construction of large number of ports and terminals for receiving ships and transferring cargos. Vertical breakwaters and sea walls are frequently used structures to protect ports from sea actions like waves and high water levels. In this regard, controlling overtopping of the waves at the top of the vertical breakwaters is a critical issue for the ship safety in the harbors. This is why engineers/designers tend to provide the vertical breakwaters with a return crown wall or even a completely horizontal cantilever slab to reduce the overtopping. However, wave impacts on the horizontal part give rise to a significant uplifting force. These forces are wave impact loads and they cannot be substituted by a static equivalent. Thereby, a detailed description of the space and time distribution of the wave impacts becomes imperative.

In the past decades, the qualitative and quantitative determination of wave loads on vertical structures has already been examined (e.g. Oumeraci et al., 2001). Uplift loads below horizontal decks have been investigated (e.g. McConnell et al., 2003) and recently prediction methods for wave loading have been developed in several research projects (e.g. Coumo et al., 2007). Contrary to the previous simple vertical wall or horizontal decks, structures consisting of both vertical parapets and horizontal cantilevering slabs have scarcely been considered. A consensus on the necessary approach for the research of this type of structures lacks completely (Okamura 1993). In addition, the structure prevents most of the overtopping due to its particular geometry - involving closed angles, which do not allow incident waves to dissipate- the loading condition is more severe than the preceding situations.

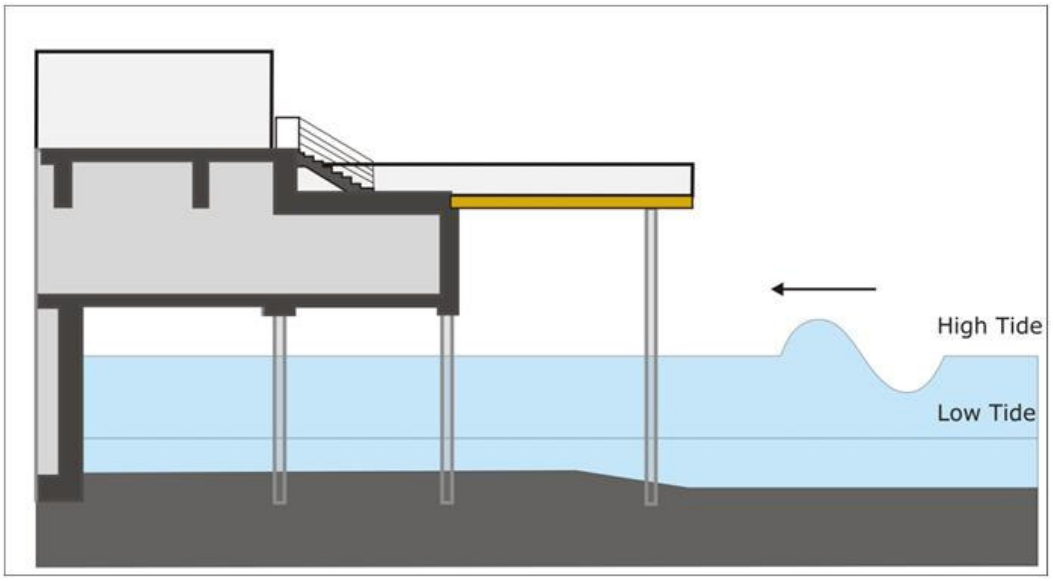

Figure 1. Schematic view of Blankenberge Pier

[1] Department of Civil Engineering, Ghent University, Technologiepark 904, Ghent, 9052, Belgium

The Pier of Blankenberge which is located along the Belgian coast is an illustrative example of a vertical wall with an overhanging horizontal cantilever slab (see fig. 1). Throughout high tides and storms, the structure is exposed to violent wave impacts, including waves running up against the vertical wall and slamming on the horizontal part. In Verhaeghe et al. (2006) a description of the field monitoring equipment installed on the pier for measuring wave loading has been provided.

The main objective of the present research, is to bring a new design tool to assess violent water wave impacts on a vertical wall, including an overhanging horizontal cantilever slab, based on the correlation between the kinematics of breaking waves and the height, distribution, duration and characteristics of the violent wave impacts. In this particular research, small scale model tests were carried out to fulfill the above goals.

Within this paper, an overview of the small scale model tests set up will be provided. This will be followed by the parametric analysis of measured forces and pressures both on the vertical and horizontal part of the scaled model. Based on the discussion of the test results, conclusions will be formulated.

EXPERIMENTAL SET-UP

Physical model tests are carried out in the wave flume (30 m x 1 m x 1.2 m) of Ghent University in Belgium. The model is located 22.5 m away from the wave paddle on a uniform slope with 50 cm depth at the location of the structure. The model is 30 cm high and 60 cm long. The foreshore slope is 1/20 (see Fig. 2).For more details see Kisacik et al. (2008).

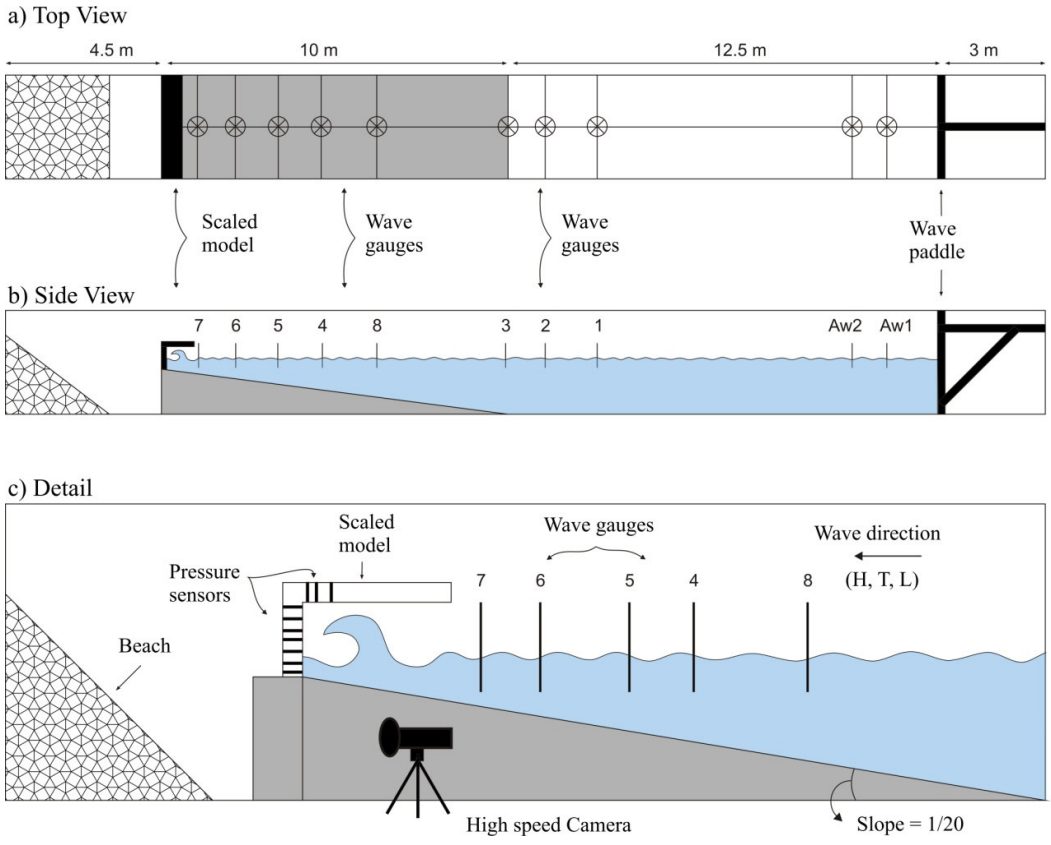

Figure 2. Small-scale model set up. a) is the top view, b) is the side view and c) is detailed view of model.

The physical model is built from a transparent plastic material and instrumented with 10 sets of pressure sensors, 9 sets of wave gauges and a high speed camera (HSC). Figure 3 shows photos of the instrumentation and the scaled model used in the tests.

The high speed camera is used to record the development of waves before breaking on the structure as a function of time. The camera provides information on the breaking mechanism of waves and shape of impact which helps to determine the types of breaking. For this purpose, an ultima APX-RS FASTCAM camera is used. It is able to deliver images up to 250 000 frames per second (fps) and has full mega pixel resolution at 3000 fps with maximum 16 GB storing capacity. In this study, it has been used at 250 fps, limited by the duration of the record. Because of the high frame rate, the camera shutter time is extremely short. In order to overcome low illumination, special flicker free lights have been used. The background is painted black to have a good contrast on the shape of the recorded free surface.

In addition, 10 sets of pressure sensors are used to register wave impact pressures as a function of time. These are quartz pressure sensors developed for measuring dynamic and quasi-static pressures with external amplifiers. The measurement range for this device is up to 200 kPa and they measure within temperature range up to 200^0 C. A sampling frequency of 20 kHz is used for the pressure recording. Such high sampling frequencies are required, since the pressure peaks occur in a very small time interval (order of magnitude milliseconds). For the same reason the natural frequency of the sensors should be high enough and a natural frequency of 150 kHz was considered. Besides that, a small pressure cell diaphragm area is necessary since the pressure peaks are also very much localized in space and the used one has a cell with a small diaphragm of 5.5 mm. Even pressure cells with diameter 5.5 mm might measure a space-averaged pressure, which is slightly different from the peak pressure. Consequently the sensors are very well suited for measuring impact phenomena.

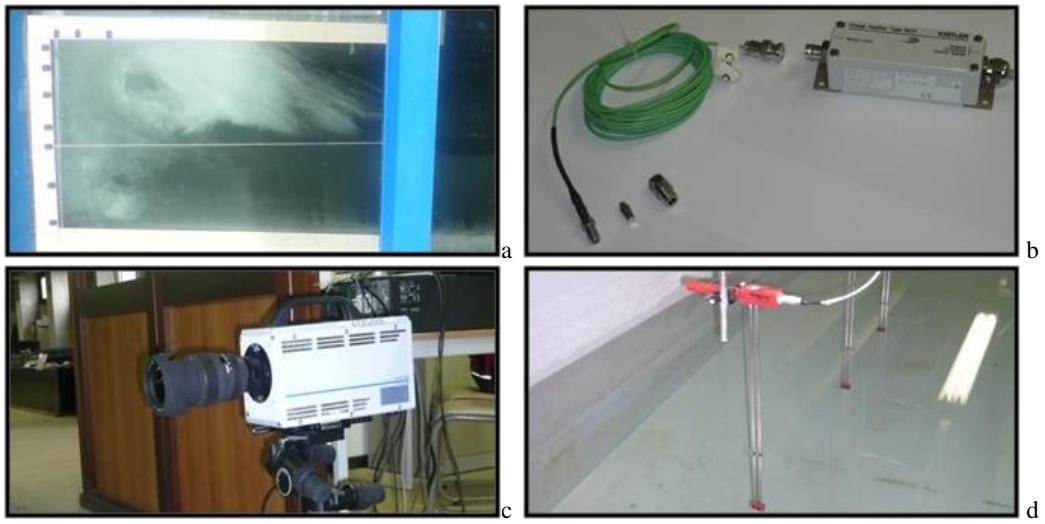

Figure 3. Picture of scaled model and used instrumentations. a) Scaled model, b) Pressure sensors, c) High Speed Camera (HSC), d) Wave gauges.

The sensors are flushmounted. Mounting adapters are used to fix the sensors on the model. These adapters are avoiding the external lateral pressure due to the bending or / and deformation of the installation holes.

For the synchronization of all instruments, wave gauge mounted at the toe of the foreshore serve as a trigger for the data acquisition system. When the first wave reaches the gauge, the recording of the pressure sensors, wave gauges and camera signal starts automatically.

Figure 4 shows the configuration of the pressure sensor holes, both on the vertical and horizontal parts of the scaled model. The accuracy of the pressure profiles mainly depends on the spatial resolution of the pressure sensors, since two rows of pressure sensor holes are distributed along the centerline with a uniform interval of 3 cm. Due to the problem of material stability and installation difficulties, it is difficult to open holes closer than 3 cm. The second row is therefore shifted 1.5 cm to achieve a uniform sensor interval of 1.5 cm along the centerline. This configuration gives flexibility to define the sensor positions as close as 1.5 cm to each other.

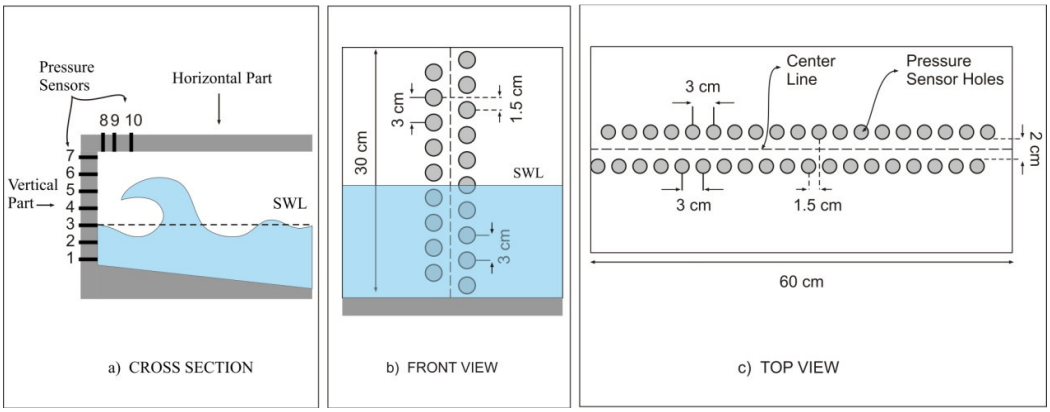

Figure 4. Detail of scaled model and configuration of pressure sensor locations

It is important to measure wave impact pressure simultaneously both on the vertical and horizontal part of the scaled model, since measured peak pressure values show a significant scatter even under the same hydrodynamic conditions. In this respect, distributions of sensor locations are becoming quite important because of the fact that we have only 10 pressure sensors. Due to the limited number of pressure sensors, tests are repeated by changing the sensor location to complete the high resolution pressure profile. During the repeated tests, sufficient overlaps between series of measurements are considered. From the measured complete pressure profile, critical sensor positions are selected. Figure 5 represents the measured peak pressure values per impact from all sensor locations on both the vertical and horizontal part. From the results of these measurements, seven positions on the vertical part and three positions on the horizontal part are selected as the critical sensor positions for further measurements. Results of the selected positions are shown in red. The above procedure is repeated for the other water depths to define the critical sensor locations.

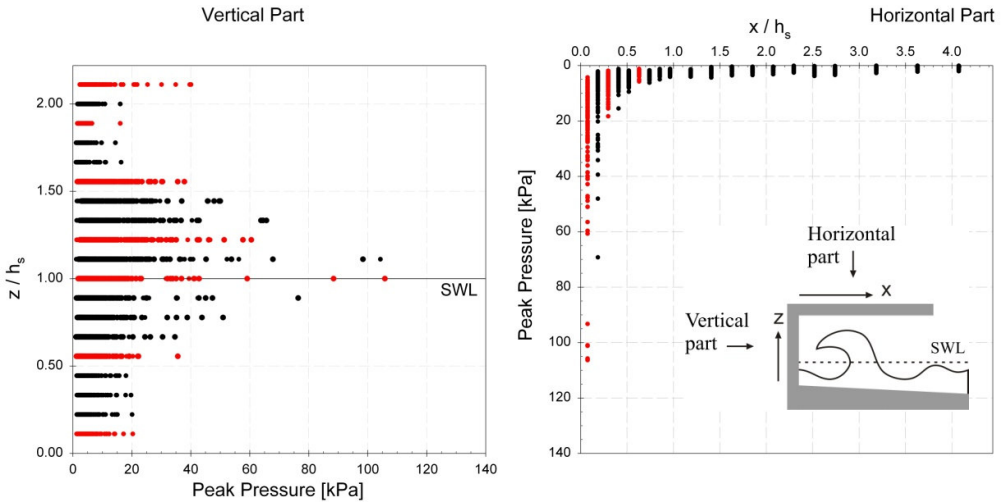

Figure 5. Peak pressure distribution both on the vertical and horizontal part for thirty regular waves ($h_s = 0.135\ m$, T=2.2 s, sampling frequency=20 kHz and H=0.115 m).

The scaled model is tested under the test parameter matrix. Tests are carried out for 18 regular waves and each test was repeated. In addition, wave heights are measured at various locations such as like 5 wave heights before the structure. In the model tests, the wave period (T), incident wave height (H) and water depth (h_s) are considered as variable input parameters. Tests are conducted for four different values of water depth and wave period. For each combination of parameters, wave heights ranging from non breaking to broken waves are considered. The matrix of parameters is summarized in Table 1.

Table 1. Test parameter matrix.

Water depth at the structure h_s (m)	Wave period T (s)	Wave height H range (m)
0.075	2.2	0.034-0.080
0.105	2.2	0.044-0.139
0.135	2.2, 2.4, 2.6, 2.8	0.059-0.168
0.165	2.2	0.075-0.191

The total horizontal and vertical forces on the scaled model are calculated by integrating the pressure results (Eq. 1 and Eq. 2).

$$F_h(t) = 0.5 \sum_{k=1}^{n-1} [p_k(t) + p_{k+1}(t)] * \Delta z_k \quad (1)$$

$$F_v(t) = 0.5 \sum_{j=1}^{m-1} [p_j(t) + p_{j+1}(t)] * \Delta x_j \quad (2)$$

Where $p_k(t)$ and $p_j(t)$ are the measured instantaneous pressure at the locations of the k-th and j-th sensors, Δz_k and Δx_j are the distances between two sensors and n and m are the number of sensors on the vertical and horizontal part, respectively.

RESULTS

The number of waves in one test is limited to 18 since lateral movement commences, due to high reflection. The first and last two wave results are removed from the analysis to have a uniform data set. Figure 6 shows an example of forces recorded on the horizontal and vertical parts of the scaled model. Although the waves in each sample are nominally identical, their impact behavior varies significantly. The non repeatability of the breaking wave impact pressures and forces on the vertical structures are a well known phenomenon and reported by many researchers [Bagnold (1939); Chan & Melville (1988); Chan (1994); Hattori et al. (1994); Kirkgoz (1995); Peregrine (2003); Bullock et al. (2007)]. From literature, the main reasons for the non repeatability are listed below.

- Turbulence left behind by a preceding wave
- Strong interaction with the reflection of the preceding wave
- Influence of trapped air

These parameters have a strong influence on the breaking wave kinematics and on the shape of the waves which has a strong relation to the value of peak pressures. Moreover, the resolution of sensor locations and the sampling frequency of the sensors influence the results.

Furthermore, the ratio between measured horizontal and vertical forces (F_h/F_v) displays scatter. In addition, the parameters affecting wave impact on the vertical part (this is the first impact) as well as the parameters influencing the second impact on the horizontal part are both reasons for this secondary scatter. These parameters are the impact shape of the rising jet (shape of the second impact) on the vertical part and the amount of air in this jet.

As mentioned previously the shape of the breaking wave has a significant consequence on the wave impact pressure and the shape which creates the largest pressure is uncertain. In this context, some of the breaking shapes are discussed and suggested in the literature. One of the first literature suggestion was made by Bagnold (1939). He described the breaking shape as a very flat vertical wave front, enclosing a thin cushion of air between itself and the wall. However, Kirkgoz (1982) defined perfect breaking when waves strike on a vertical wall with a perfectly vertical face. This has not been confirmed by Hull and Muller (2002). Furthermore, researchers like Bullock et al. (2007), Partenscky (1988) and Hattori et al. (1994) showed that the largest impact pressures occur when the breaking wave trapped a very thin pocket of air. Oumeraci et al. (1995) found that a plunging breaker with a large air pocket causes the highest pressures. In addition, Chan and Melville (1988) observed that wave impact occurred through the focusing of the incident wavefront on to the wall. This argument is supported by theoretical work conducted by Peregrine (1994) as well.

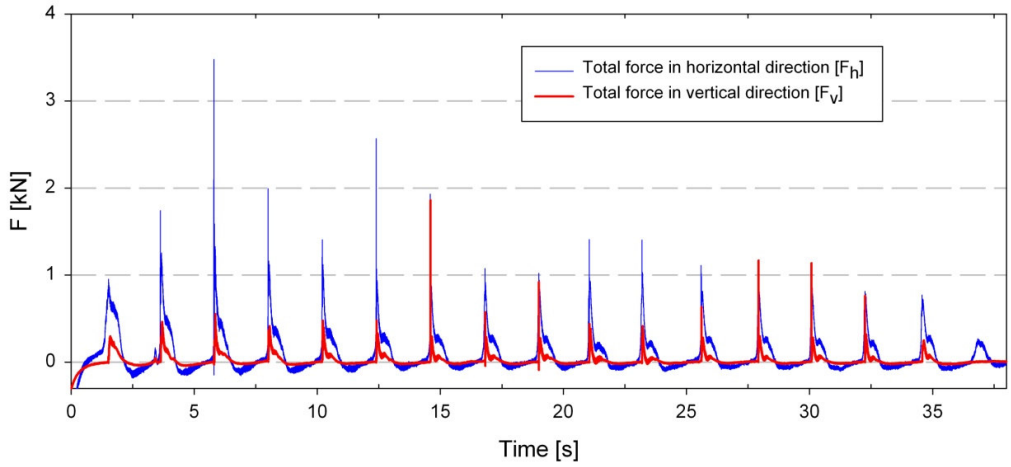

Figure 6. An example of measured vertical and horizontal forces for 18 individual wave impacts (h_s = 0.135 m, T=2.2 s, sampling frequency=20 kHz and H=0.11 m)

In this particular research, it is observed that the breaker with a small air trap gives rise to the highest pressures. A sequence of HSC images for breaking with a small air trap is demonstrated in Figure 7. It is also meaningful to mention the amount of trapped air is a subjective observation based on the slow motion HSC results. The shape of the secondary impact occurring on the overhanging part is also important for the amount of the pressure at the corner of the scaled model. This will be either in spray form or a jet climbing on the vertical part. This jet may contain air depending on the type of the impact on the vertical part.

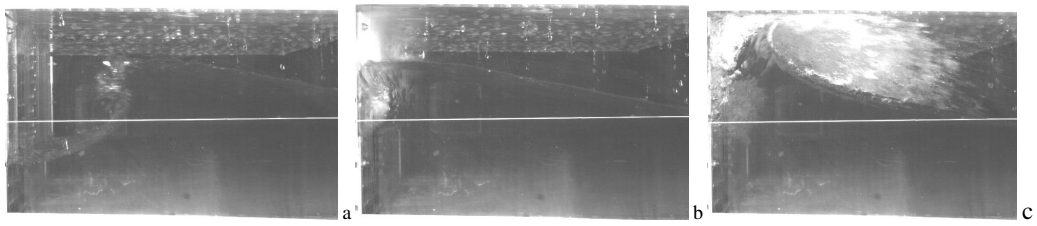

Figure 7. From left to right: sequence of HSC images illustrating the evolution of the free-surface during the impact. White line at the middle represents the SWL.

The magnitude of the maximum pressure (p_{max}) and its distributions are critical issues for design engineers. From previous laboratory investigations, researchers found that on vertical structures the location of p_{max} varies in an interval around SWL. Richert (1968) found the p_{max} below the SWL. However, Hattori et al. (1994), Hull and Muller (2002) and Oumeraci et al. (1995) found the p_{max} at the SWL. In addition, some others like Kirkgöz (1982), Partenscky (1988), Chan & Melville (1988) and Bullock et al. (2007) found the p_{max} above the SWL. Figure 8 shows local peak pressure distribution both on the vertical and horizontal parts for $h_s = 0.105$ m. It is observed that the location of p_{max} is above SWL (order of distance is one wave crest height). However, for $h_s = 0.135$ m the p_{max} values are measured at SWL (see fig. 5). On the horizontal part, the maximum pressure location is at the corner of the horizontal part. Further away from the corner, p_{max} values are exponentially decreasing. Kisacik et al. (2010) found that the largest peak pressures are recorded at the SWL ($82 * \rho g h_s$) on the vertical part and at the corner of the horizontal part ($90 * \rho g h_s$), where, ρ is the density of the water and g is the acceleration of gravity.

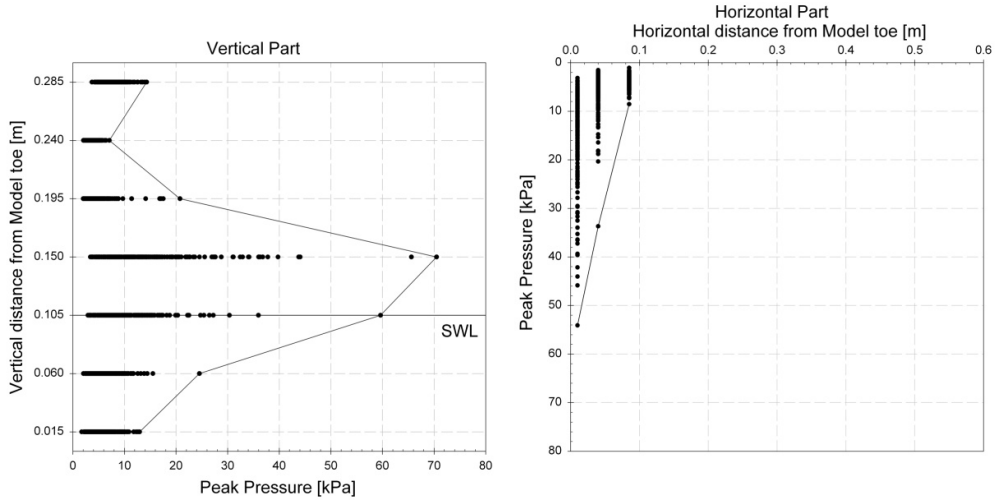

Figure 8. Peak pressure distribution both on the vertical and horizontal part for thirty regular waves (, T=2.2 s, sampling frequency=20 kHz).

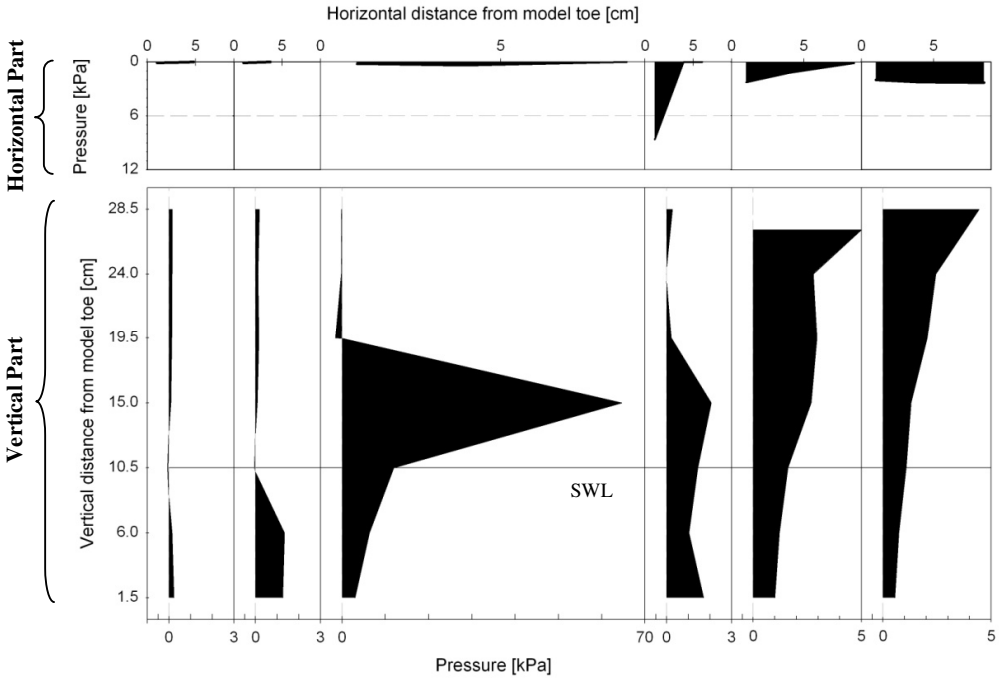

Figure 9. Instantaneous pressure distribution both on vertical and horizontal parts for several different time instants. Time interval between the sections

Figure 9 illustrates an example of the instantaneous pressure distribution both on vertical and horizontal parts for several different time instants. On the lower figure, x and y axis show the instantaneous pressure in kPa and the vertical distance from the model toe respectively while the upper figure represents the pressure distribution on the horizontal part. From left to right, figures show the evolution of the pressure distribution. The third and fourth profiles represent the instantaneous pressure distribution at the time of the maximum horizontal and vertical pressures. There is a phase difference between the maximum of horizontal and vertical forces, which is essentially important for overturning moment of calculations.

Variation of wave height (H)

In accordance with Oumeraci et al., (1993), the wave impact pressure characteristics are divided into four principal categories in relation to the following breaker shapes: slightly breaking waves, breaking with small air trap, breaking with large air trap, and broken waves.

Figure 10 represents the variation of maximum forces (F_h and F_v) on the vertical and horizontal part with the variation of wave height (H) at the toe of the foreshore. On the figures, the dots with blue, red and black colors illustrate measured forces in the slightly breaking, breaking and broken wave zones, respectively.

As seen on the figure, horizontal force (F_h) displays a high scatter in the breaking wave zone (0.95 m<H<0.16 m) and this scattering region extends to the slightly breaking and broken wave zone (0.75 m<H<0.16 m) for the measured vertical forces (F_v). In these zones, rising water columns on the vertical part resulting in high impact loads on the horizontal part. Therefore, on the horizontal part the range of wave height which creates impact loads is larger than the wave height range creates impact on the vertical part.

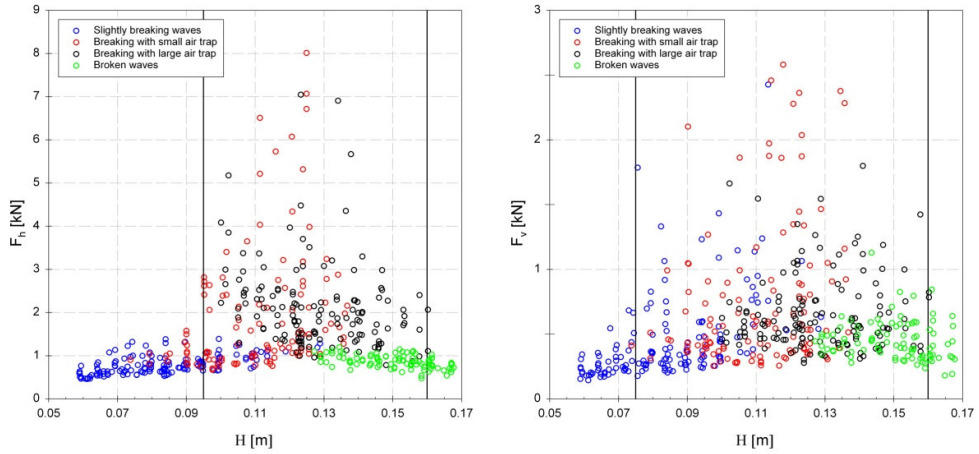

Figure 10. Variation of measured maximum force values with the change of wave height (H) measured at the toe of the foreshore.

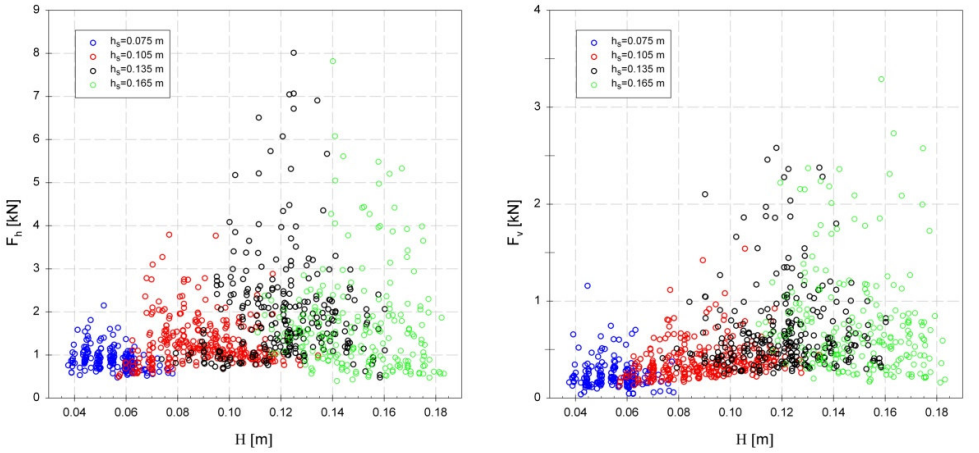

Figure 11. Variation of measured maximum force values with the change of water depth (h_s) measured at the toe of the scaled model.

Variation of water depth (h_s)

Figure 11 displays the variation of both measured maximum force values (F_h and F_v) with the variation of water depth (h_s) at the toe of scaled model for the case of breaking waves. Each different color represents the results of a different water depth. The present results show the magnitude of the maximum impact pressures and forces decrease rapidly as the ratio of wave height to water depth (H/h_s) becomes smaller or larger than a certain value (See fig. 10). Therefore, instead of a fixed wave height, wave height range $0.7 < H/h_s < 1.1$ is considered for each different h_s. Measured force values are very sensitive for the variation of h_s and increasing h_s results in a high impact force both on the horizontal and vertical part of the scaled model.

However, some low results in the highest water level case ($h_s = 0.165\ m$) are observed. In this water level, some of the waves are hitting on the horizontal part when they are developing to break and this is blocking the waves to create high impact forces.

Variation of wave period (T)

Figure 12 illustrates the variation of both measured maximum force values (F_h and F_v) with the variation of wave period (T) at the toe of the foreshore for the case of breaking waves. Each different color represents the results of a different wave period. Same wave height ranges, as used in the variation of h_s case are being considered. As it is seen in fig. 12, measured maximum force values display a dependency on the variation of the wave period (T). However, looking at the best lines of the data cloud, the change in terms of wave period has a rather limited effect on the measured forces.

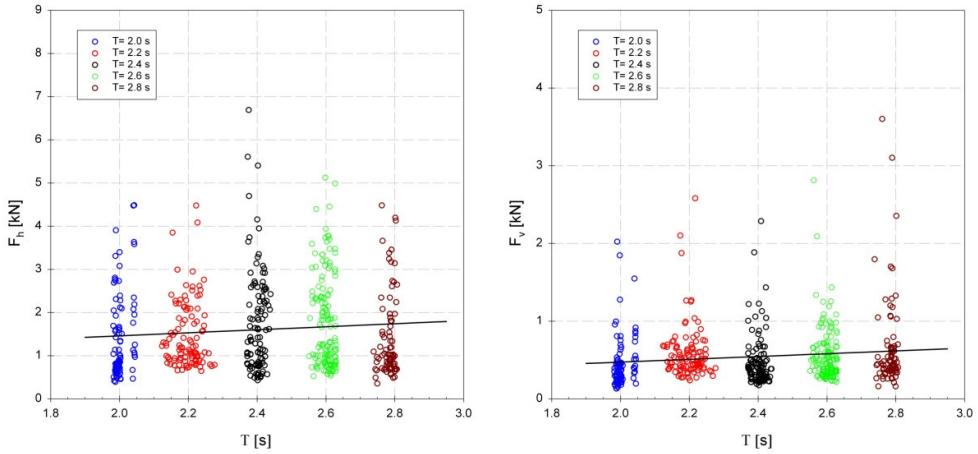

Figure 12. Variation of measured maximum force values with the change of wave period (T) measured at the toe of the foreshore.

CONCLUSIONS

A vertical wall with horizontal cantilevering slab is tested in a small scale test set-up (at scale 1:20) using regular waves for four different values of water depth and wave period. All the events have been recorded by a high speed camera with 250 frames per second. Pressures on the models have been measured by 10 pressure sensors using 20 kHz sampling frequency. A parametric analysis of measured forces and pressures both on the vertical and horizontal part of the scaled model is conducted. Resulting from the experiments, the following conclusions are drawn:

- The highest impact pressure and forces are measured in the case of breaking waves with small air trap.
- The location of p_{max} is varying between SWL and a distance one wave crest above SWL on the vertical part while it is observed at the corner of the scaled model on the horizontal part.
- In the slightly breaking and broken wave zones, rising water columns on the vertical part are resulting in high impact loads on the horizontal part. Therefore, the horizon part exposes to impact waves more than the vertical part.

- Measured forces are very sensitive for the variation of water depth (h_s) and increasing h_s results in a high impact force both on the horizontal and vertical part of the scaled model.
- Variation of wave period (T) has a rather limited effect on the measured forces compared to variation of h_s and H.

ACKNOWLEDGMENTS

This study has been supported by the Special Research Fund by Ghent University (BOF). The support of funding for new instruments by Research Foundation-Flanders (FWO) is also gratefully acknowledged.

REFERENCES

Bagnold, R. A. (1939), '*Interim report on wave-pressure research'*, Proc. Inst, Civil Eng. 12, 201–226.

Bullock, G.N.; Obhrai, C.; Peregrine, D.H.; Bredmose, H. (2007) '*Violent breaking wave impacts. Part 1: Results from large-scale regular wave tests on vertical and sloping walls' C*oastal Engineering, v 54, n 8, p 602-617, August 2007

Chan, E. (1994) '*Mechanics of deep water plunging-wave impacts on vertical structures'* Coastal Engineering, v 22, n 1-2, p 115-133, Jan 1994

Chan, E.S. and Melville, W.K., (1988) '*Deep-water plunging wave pressures on a vertical plane wall'*, Proc. Roy. Soc. London, A, 417(1852), 95-131.

Cuomo G.; Tirindelli M.; and William Allsop W., 2007, '*Wave-in-deck loads on exposed jetties*', Coastal Engineering Volume 54, Issues-9, 2007, pp: 657-679

Hattori, M. ; Arami, A. ; Yui, T. (1994) '*Wave impact pressure on vertical walls under breaking waves of various types*' Coastal Engineering, v 22, n 1-2, p 79-114, Jan 1994

Hull, P.; Müller, G. (2002) *'An investigation of breaker heights, shapes and pressures'* Ocean Engineering, v 29, n 1, p 59-79, September 21, 2002

Kirkgoz, M.S. (1995) '*Breaking wave impact on vertical and sloping coastal structures'* Ocean Engineering, v 22, n 1, p 35-48, Jan 1995

Kirkgoz, M.Salih (1982) *'Shock pressure of breaking waves on vertical walls.'* Journal of the Waterway, Port, Coastal and Ocean Division, v 108, n WW1, p 81-95, Feb 1982

Kisacik, D.; Verleysen, P.; Van Bogaert, P.; Troch, P. (2010) *'Comparative Study on Breaking Wave Forces on Vertical Walls with Cantilever Surfaces'* The Proceedings of The Twentieth (2010) International Offshore and Polar Engineering Conference Beijing, China, June 20-25, 2010

Kisacik, Dogan; Van Bogaert, Philippe; Troch, Peter; Van Slycken, J. (2008) '*Experimental results of loading conditions due to violent wave impacts on coastal structures with cantilever surfaces'*, Second International Conference on the Application of Physical Modelling to Port and Coastal Protection (CoastLab '08), July 2-5, 2008, Bari, Italy, pp. 587-598, ISBN: 978-90-78046-07-3

McConnell, K.J; Allsop, N.W.H; Cuomo, G; and. Cruickshank, I.C, 2003, *'New guidance for wave forces on jetties in exposed locations*', Paper to Conf. COPEDEC VI, Colombo, Sri Lanka pp: 20

Okamura, M., 1993, '*Impulsive pressure due to wave impact on an inclined plane wall'*, Fluid Dynamics Research, volume 12, issue 4, pp. 215-228

Oumeraci, H.; Bruce, T.; Klammer, P.; Easson, W.J. (1995): PIV measurement of breaking wave kinematics and impact loading of caisson breakwaters. COPEDEC, no. 4, v 3, pp. 2394-2410.

Oumeraci, H.; Klammer, P.; Partenscky, H.W. (1993) *'Classification of breaking wave loads on vertical structures'* Journal of Waterway, Port, Coastal and Ocean Eng. v 119, n 4, p 381-397

Oumeraci, H; Kortenhaus, A; Allsop, W; de Groot, M; Crouch, R; Vrijling, H; Voortman, H, 2001, "*Probabilistic Design Tools for Vertical Breakwaters*", Balkema Publishers, New York.

Partenscky, H. (1988) *'Dynamic forces due to waves breaking at vertical coastal structures'* Twenty First Costal Eng Conf, p 2504-2518, 1988, Twenty First Costal Eng Conf

Peregrine, D.H. (2003) '*Water-wave impact on walls'* Annual Review of Fluid Mec. v 35, p 23-43

Peregrine, D.H.; Topliss, M.E. (1994) *'Pressure field due to steep water waves incident on a vertical wall'* Proceedings of the Coastal Engineering Conference, v 2, p 1496-1510, 1995

Richert, G., (1968) '*Experimental investigation of shock pressures against breakwaters'*. In: Proc. Int. Conf. Coastal Engng, ASCE, London, pp. 954–973.

Verhaeghe, H.; Cherlet, J.; Boone, C.; Troch, P.; De Rouck, J.; Awouters, M.; Ockier, M.; Devos, G., 2006, '*Prototype monitoring of wave loads on concrete structure in intertidal zone*', COASTLAB06. pp. 117-125